High-Pressure Study of X-Ray Diffuse Scattering in Ferroelectric Perovskites

Sylvain Ravy,[1] Jean-Paul Itié,[1,2] Alain Polian,[2] and Michael Hanfland[3]

[1]*Synchrotron SOLEIL, L'Orme des merisiers, Saint-Aubin BP 48, 91192 Gif-sur-Yvette cedex, France*
[2]*Physique des Milieux Denses, IMPMC, CNRS UMR 7590, Université P. et M. Curie, 140 rue de Lourmel, 75015 Paris, France*
[3]*European Synchrotron Radiation Facility, 6 rue Jules Horowitz, Boîte postale 220, 38043 Grenoble Cedex, France*

(Received 27 April 2007; published 14 September 2007)

We present a high-pressure x-ray diffuse scattering study of the ABO_3 ferroelectric perovskites $BaTiO_3$ and $KNbO_3$. The well-known diffuse lines are observed in all the phases studied. In $KNbO_3$, we show that the lines are present up to 21.8 GPa, with constant width and a slightly decreasing intensity. At variance, the intensity of the diffuse lines observed in the cubic phase of $BaTiO_3$ linearly decreases to zero at ~11 GPa. These results are discussed with respect to x-ray absorption measurements, which leads to the conclusion that the diffuse lines are only observed when the B atom is off the center of the oxygen tetrahedron. The role of such disorder on the ferroelectric instability of perovskites is discussed.

DOI: 10.1103/PhysRevLett.99.117601 PACS numbers: 77.84.Dy, 61.10.−i, 61.50.Ks, 62.50.+p

Because of the simplicity of their structure and their actual or potential applications, perovskites ABO_3 and their derivatives are amongst the most studied compounds in solid state science. Perovskites stabilize a large variety of states such as superconductivity, ferroelectricity (FE), and multiferroism, but despite decades of studies, the mechanisms of these transitions are still a matter of debate [1]. This is the case of the oxygen perovskites such as $SrTiO_3$ and $KTaO_3$, which only exhibit incipient FE, while $PbTiO_3$, $BaTiO_3$, and $KNbO_3$ stabilize this instability in well-defined series of FE transitions.

Upon heating at ambient pressure, barium titanate and potassium niobate undergo the same famous sequence of rhomboedric-orthorhombic-tetragonal-cubic (R-O-T-C) first-order phase transitions [2,3]. During this sequence, the polarization changes direction from the [111], to the [110] and [100] pseudocubic directions, before vanishing above the Curie temperature T_C in the cubic phase. The mechanism of this sequence of phase transitions has been often discussed from two limiting cases: the soft-mode—or displacive—theory, in which a transverse optical (TO) mode gradually softens when approaching the phase transition [4], and an order-disorder scenario [5], in which some atoms lying on symmetry-equivalent sites order on preferential ones. In fact, current theories favor an intermediate situation, in which soft phonons and disorder play a role [6,7].

Pressure has proven to be an essential parameter to study phase transitions in perovskites [8]. Because applying pressure results in a symmetrization of chemical bonds, drastic effects on order-disorder phase transitions are expected. Indeed, the same sequence of phase transitions is observed as a function of pressure in $KNbO_3$ and $BaTiO_3$ [9]. At 300 K, FE is lost at 10 GPa (2 GPa) and is no more observed at low temperature above ~26 GPa (~6.5 GPa) in $KNbO_3$ ($BaTiO_3$). The existence of the O-T transition under pressure has been questioned in $KNbO_3$ [10], while in other studies its transition pressure was found at 6 GPa [11] or 8.5 GPa [9]. In this Letter, we will show that high-pressure x-ray diffuse scattering measurements give a unique opportunity to study the transitions and the FE instability as a function of the nature and the position of the B atom.

The fluctuations leading to the FE state are complex, as demonstrated by the numerous and apparently conflicting experimental results gathered for decades. After the first observation of diffuse lines (DL) by electron [12] and x-ray diffraction [13] in barium titanate, Comès *et al.* [3] performed a thorough study of the DL in potassium niobate and showed that they are due to reciprocal diffuse {100} *sheets* [see Fig. 1(a)] intersecting the Ewald sphere. There are three sets of sheets in the C phase, two sets in the T phase [(010) in red and (100) in orange], one in the O phase (010), and no DL in the low temperature R phase. Measured far from the Bragg positions, the intensity and the width of the lines are constant in a given phase [14].

Comès *et al.* interpreted the DL from the so-called "8-sites" model [15] in which the B atom is locally dis-

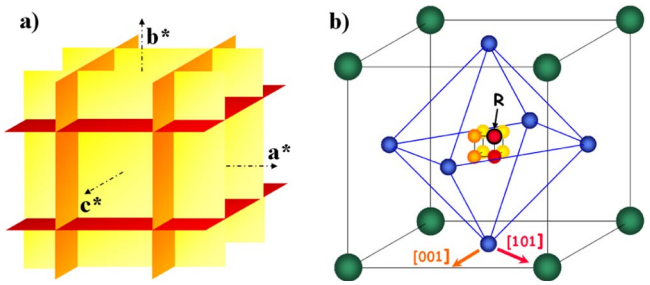

FIG. 1 (color online). (a) Schematic representation of the diffuse sheets in the reciprocal space. The color scheme corresponds to the sites occupancy shown in (b). (b) Perovkites pseudocubic unit cell and the 8 sites of the Ti/Nb atoms. The R, red, red-orange, and red-orange-yellow sites are occupied in the R, O, T, and C phases, respectively. For the sake of consistency with previous studies, we take the b axis vertical, and c along the x-ray beam.

placed from the center of the unit cell along the ⟨111⟩ directions [see Fig. 1(b)]. This model was actually very efficient in explaining the sequence of phase transitions by the successive ordering of the B atoms on 4, 2, and 1 sites in the T, O, and R phases, respectively. The DL were shown to be due to independent linear correlations of each components of the Nb (Ti) displacement.

To explain these results, Hüller [16] proposed an alternative model based on the presence of highly anisotropic TO soft mode. In fact, inelastic neutron scattering (INS) revealed a more complex and phase-dependant origin of the DL. In O-$KNbO_3$, Currat *et al.* [17,18] clearly evidenced (i) a highly anisotropic transverse acoustic (TA) branch with a flat dispersion at ~1.6 THz in the diffuse scattering plane and (ii) a well-defined soft TO mode with similar anisotropy. This gave a clear support to the soft-mode interpretation, at least in the O phase. At variance, in C-$KNbO_3$ [19] and in C-$BaTiO_3$ [20] an anisotropic and highly *overdamped* TO mode was observed, which was rather interpreted in the order-disorder framework.

Inelastic light scattering results [21–23] complexified this picture, by evidencing a "central peak" owing to a relaxational mode, in O-, T-$KNbO_3$, T-, and C-$BaTiO_3$. This mode was interpreted from the 8-sites model as due to thermally activated jumps between *unsymmetrical* [22,23] positions of the Ti or Nb atoms.

Results from local probes techniques like EPR [24], NMR [25], or x-ray absorption fine structure (XAFS) [26–28], also support the 8-sites model. In particular, it was found by EXAFS in all the phases of $KNbO_3$ [26] that Nb is shifted by $u \sim 0.2$ Å with respect to the oxygen octahedron, in the [111] direction. This value is consistent with the displacements measured in the ordered phases [2]. In the case of $BaTiO_3$, a preedge peak at the Ti K edge, whose intensity is partly proportional to $\langle u^2 \rangle$ [29], was studied as a function of the x-ray polarization, which led to the same conclusion [27]. Thus, whatever the actual type of dynamics, these XAFS results show that in the paraelectric phase, the Ti(Nb) atoms spend more time at the [111] sites than at any other sites of the unit cell, including its center.

Most interesting is the recent evidence by XAFS measurements that in $BaTiO_3$ the Ti atom moves and locks on to the center of the oxygen octahedron above 10 GPa [30], at variance with $KNbO_3$, where the Nb atom does not reach the central position up to 15.8 GPa [28]. This stimulated us to carry out high-pressure x-ray diffuse scattering experiments on $KNbO_3$ and $BaTiO_3$.

The experiments have been performed at the ID09A beam line of the European Synchrotron Radiation Facility (ESRF), using a membrane diamond anvil cell (MDAC) [31]. The 30×30 μm^2 30 keV beam was vertically focused by a spherical mirror and horizontally by a bent silicon (111) monochromator. All the diffraction patterns presented here were collected by a Mar345 image-plate detector, using 2° oscillations of the crystal about the vertical axis on a −15° to 15° angular domain.

A first $KNbO_3$ single crystal was loaded in the hole of a stainless steel gasket (initial diameter $\Phi = 150$ μm, initial thickness $e = 52$ μm), with Ne as pressure-transmitting medium and a ruby sphere as pressure probe. Typical diffraction patterns are shown on Fig. 2(a)–2(c). In this MDAC, the maximum measurable scattering vector was $q \sim 5$ Å^{-1}. As this crystal broke at about 13 GPa, a second single crystal was mounted in a He-loaded MDAC (maximum $q \sim 6.2$ Å^{-1}), with a stainless steel gasket ($\Phi = 250$ μm, $e = 80$ μm). This mounting allowed us to keep the crystal integrity up to 21.8 GPa [Fig. 2(d)]. The $BaTiO_3$ single crystal was loaded in the hole of a Rh gasket ($\Phi = 120$ μm, $e = 70$ μm) with methanol-ethanol-water (16:3:1), in the first type of MDAC.

The diffraction patterns of $KNbO_3$ displayed in Fig. 2 clearly show the presence of {001} DL in all the phases. The signal-to-noise ratio for the DL was found to be about 10%, probably because of the diamond Compton scattering. In the O phase, (010) DL are visible up to $k = 3$, with similar characteristics as first reported in [3]: absence of $k = 0$ lines and half width at half maximum (HWHM) equal to ~0.08 Å^{-1} (1/20 of the BZ). By increasing the pressure below ~6 GPa [Fig. 2(a)], very weak (100) DL can be detected. Between ~6 GPa and ~10 GPa [Fig. 2(b)], the second set of (100) DL becomes visible and appears to be stronger than the (010) set. This result was observed on the two samples. Above 10 GPa [Fig. 2(c)], the two sets of (010) and (100) DL are present with the same intensity, indicating the stabilization of the C phase, consistently with the results of Refs. [9–11]. Note that in the C phase the set of (001) DL should be visible, but a look to Fig. 6(a) of Ref. [3] makes it clear that these DL are weaker and only apparent at the $h, k = 4$ DL level.

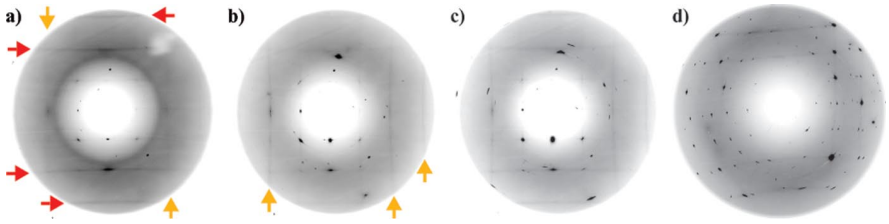

FIG. 2 (color online). Scattering patterns of $KNbO_3$ (no. 1) at (a) 4.3 GPa, (b) 6.3 GPa, and (c) 12.1 GPa. Red and orange arrows point to (010) and (100) diffuse lines, respectively. The background and the diffuse ring in (a) are due to the scattering by liquid Ne. (d) Diffraction pattern of $KNbO_3$ (no. 2) at 21.8 GPa.

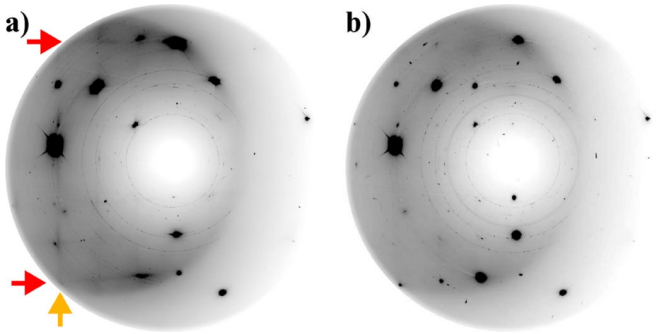

FIG. 3 (color online). Scattering patterns of $BaTiO_3$ at (a) 2.6 GPa and (b) 11.3 GPa. Red and orange arrows point to (010) and (100) diffuse lines, respectively. The contrast has been increased, which makes the diffuse lines more visible and the Bragg spots more intense than in Fig. 2.

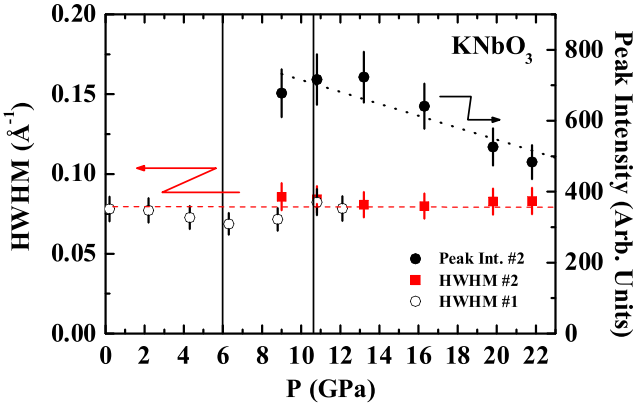

FIG. 4 (color online). Pressure dependence of the peak intensity (right scale) and the HWHM (left scale) of the diffuse lines of $KNbO_3$ [sample 1 (2), open (full) symbols]. Lines are guides for the eye. Vertical lines indicate the *O-T* and *T-C* transition pressures, according to this study.

These levels were unreachable in our geometry. The observation of a change above 6 GPa and 10 GPa in both samples clearly indicates phase transitions, that we assign to *O-T* and *T-C*, in agreement with [11]. However, the unexpected relative intensity of the DL may indicate an unusual orientation of the tetragonal domains.

The behavior of the HWHM and the intensity of the $k = 3$ DL is indicated in Fig. 4. Only the intensity measured on sample 2 is shown, due to the difficulty of normalization between different samples. These graphs show that (i) the HWHM ~ 0.08 Å^{-1} is constant throughout the explored pressure range and (ii) the intensity slowly decreases at high pressure.

Typical diffraction patterns in $BaTiO_3$ are displayed on Fig. 3. As already noted in previous studies [3], the DL are weaker in $BaTiO_3$ than in $KNbO_3$. Moreover, they appear to be less intense near the ZB boundary than in the ZB center [32]. The pressure dependence of the intensity and the HWHMs of the DL [measured at the $(-3, -1.8, 0)$ reduced scattering vector] are shown in Fig. 5. The intensity decreases linearly and becomes undetectable at ~ 11 GPa, while the HWHM is slightly increasing.

Let us recall that for an atom of scattering factor f displaced by u, the total diffuse scattering intensity is proportional to $f^2\langle u^2\rangle$. $\langle u^2\rangle$ being similar in both compounds [27,28], the intensity of the $KNbO_3$ DL is clearly due to the large atomic number of Nb. Moreover, INS results have shown that despite similar anisotropy, the TA mode is less dispersive in $KNbO_3$ than in $BaTiO_3$ (see Fig. 1 in [18] and Fig. 5 in [20]). This explains the uniformity of the $KNbO_3$ DL. In $BaTiO_3$, the contribution of the TA mode is weaker near the ZB boundary.

Most interesting is to compare x-ray and XAFS results. In $KNbO_3$, the weakening of the DL under pressure corresponds to the decrease of u measured by EXAFS [28]. Even more striking is the strong correlation in $BaTiO_3$, between the vanishing of the DL at ~ 11 GPa and the saturation of the intensity of the preedge peak at the same pressure [30]. As both the DL intensity and the XANES preedge peak are proportional to $\langle u^2\rangle$, they have the same pressure dependence (nearly linear).

Our main results is to show unambiguously that the intensity of the DL is correlated with the off-centering displacements of the B atoms, as measured by XAFS. Consequently, the peculiar dynamics associated to the FE instability, and giving rise to the DL, results from the $\langle 111\rangle$ displacements of the B atom. The behavior observed in FE $PbTiO_3$, in which Ti is found to be displaced in the $\langle 100\rangle$ direction [27], while no DL were observed by x-ray scattering [33], reinforces the conclusion that the DL are due to the $\langle 111\rangle$ local displacements.

These results suggest drastic changes in the dynamics under pressure, especially in *C*-$BaTiO_3$. First, the contribution of the TA mode near the BZ boundary and of the TO mode at the zone center should decrease under pressure. We expect the TA and the TO modes to strongly harden up to ~ 11 GPa. Second, INS experiments have shown that

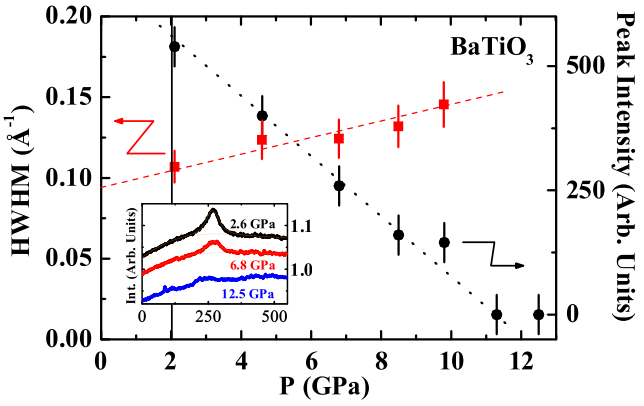

FIG. 5 (color online). Pressure dependence of the peak intensity (right scale) and the HWHM (left scale) of the diffuse lines of $BaTiO_3$. Lines are guides for the eye. The vertical line indicates the *T-C* transition pressure. Inset: profiles of the diffuse lines at 2.6, 6.8, and 12.5 GPa.

increasing the disorder makes the TO mode more and more damped. We thus expect that the centering of Ti under pressure, which decreases the disorder, makes the TO mode behave in a more harmonic way. Finally, we suggest that the relaxational mode as observed by hyperRaman [21], and probably by NMR [25,34], whose existence is due to jumps of Ti on inequivalent sites, should disappear above ~11 GPa. The present observation of a weak (100) set of DL in O-$KNbO_3$ at 4.3 GPa (also noted in [3] below the O-T transition temperature), could be the scattering signature of this mode.

Considering that the FE state is not observed above 6.5 GPa in $BaTiO_3$, it is likely that $BaTiO_3$ is an incipient FE between 6.5 and 11 GPa and $KNbO_3$ above ~26 GPa. It is thus tempting to conclude that a large enough off centering is necessary to stabilize the FE state. From the value obtained at 6.5 GPa, this threshold value can be estimated from XANES [27,30] to be $u_{Ti} = 0.1$ Å for $BaTiO_3$ and 0.08 Å for $KNbO_3$ (extrapolated at 26 GPa). Remarkably, no disorder is found in the incipient FEs $KTaO_3$ [35], and in $SrTiO_3$ recent XAFS studies conclude to 0.08 Å off centering of Ti [36], a value slightly smaller than u_{Ti}. On the theoretical side, it is noteworthy that recent *ab initio* calculations have shown that the FE instability is suppressed at ~20 GPa [37] or at ~10 GPa [38].

In conclusion, we have shown that high-pressure XAFS and x-ray scattering experiments allow one to disentangle the role of the lattice dynamics and the local order of the B atoms in the ferroelectric instabilities of perovskites. In particular, our results demonstrate that the B atom disorder enhances the FE instability and support the idea that it is an essential ingredient for the stabilization of the FE state.

We thank R. Comès, R. Currat, and B. Dorner for useful discussions.

[1] A. Gonzalo and B. Jiménez, *Ferroelectricity* (Wiley-VCH, Berlin, 2005).
[2] A. W. Hewat, J. Phys. C **6**, 2559 (1973).
[3] R. Comès, M. Lambert, and A. Guinier, Solid State Commun. **6**, 715 (1968); Acta Crystallogr. Sect. A **26**, 244 (1970).
[4] W. Cochran, Adv. Phys. **9**, 387 (1960).
[5] S. Aubry, J. Chem. Phys. **62**, 3217 (1975).
[6] Y. Girshberg and Y. Yacoby, J. Phys. Condens. Matter **11**, 9807 (1999).
[7] R. Pirc and R. Blinc, Phys. Rev. B **70**, 134107 (2004).
[8] G. A. Samara, T. Sakudo, and K. Yoshitsu, Phys. Rev. Lett. **35**, 1767 (1975).
[9] Ph. Pruzan, Int. J. Materials and Product Technology **26**, 200 (2006).
[10] Y. Kobayashi, S. Endo, T. Ashida, L. C. Ming, and T. Kikegawa, Phys. Rev. B **61**, 5819 (2000).
[11] Ph. Pruzan, D. Gourdain, and J. C. Chervin, High Press. Res. **22**, 243 (2002).
[12] G. Honjo, S. Kodera, and N. Kitamuri, J. Phys. Soc. Jpn. **19**, 351 (1964).
[13] J. Harada and G. Honjo, J. Phys. Soc. Jpn. **22**, 45 (1967).
[14] In Ref. [3], the intensity was measured at the (0, 2, 0.75) reduced scattering vector.
[15] H. Takahashi, J. Phys. Soc. Jpn. **16**, 1685 (1961).
[16] A. Hüller, Solid State Commun. **7**, 589 (1969).
[17] R. Currat, R. Comès, B. Dorner, and E. Wiesendanger, J. Phys. C **7**, 2521 (1974).
[18] R. Currat, H. Buhay, C. H. Perry, and A. M. Quittet, Phys. Rev. B **40**, 10 741 (1989).
[19] A. C. Nunes, J. D. Axe, and G. Shirane, Ferroelectrics **2**, 291 (1971).
[20] J. Harada, J. D. Axe, and G. Shirane, Phys. Rev. B **4**, 155 (1971).
[21] M. D. Fontana, A. Ridah, G. E. Kugel, and C. Carabatos-Nedelec, J. Phys. C **21**, 5853 (1988).
[22] J. P. Sokoloff, L. L. Chase, and D. Rytz, Phys. Rev. B **38**, 597 (1988).
[23] T. P. Dougherty *et al.*, Phys. Rev. B **50**, 8996 (1994).
[24] K. A. Müller and W. Berlinger, Phys. Rev. B **34**, 6130 (1986).
[25] B. Zalar, V. V. Laguta, and R. Blinc, Phys. Rev. Lett. **90**, 037601 (2003); B. Zalar, A. Lebar, J. Seliger, R. Blinc, V. V. Laguta, and M. Itoh, Phys. Rev. B **71**, 064107 (2005).
[26] K. H. Kim, W. T. Elam, and E. F. Skelton, in *Optical Fiber Materials*, edited by J. W. Fleming *et al.*, MRS Symposia Proceedings Vol. 172 (Materials Research Society, Pittsburgh, 1990), p. 291.
[27] B. Ravel, E. A. Stern, R. I. Vedrinskii, and V. Kraizman, Ferroelectrics **206**, 407 (1998).
[28] A. I. Frenkel, F. M. Wang, S. Kelly, R. Ingalls, D. Haskel, E. A. Stern, and Y. Yacoby, Phys. Rev. B **56**, 10 869 (1997).
[29] R. V. Vedrinskii *et al.*, J. Phys. Condens. Matter **10**, 9561 (1998).
[30] J.-P. Itié, B. Couzinet, A. Polian, A. M. Flank, and P. Lagarde, Europhys. Lett. **74**, 706 (2006).
[31] R. Le Toullec, J. P. Pinceaux, and P. Loubeyre, High Press. Res. **1**, 77 (1988).
[32] N. Takesue, M. Maglione, and H. Chen, Phys. Rev. B **51**, 6696 (1995).
[33] B. D. Chapman, E. A. Stern, S.-W. Han, J. O. Cross, G. T. Seidler, V. Gavrilyatchenko, R. V. Vedrinskii, and V. L. Kraizman, Phys. Rev. B **71**, 020102(R) (2005).
[34] E. A. Stern, Phys. Rev. Lett. **93**, 037601 (2004).
[35] Y. Nishihata, O. Kamishima, K. Ojima, A. Sawada, H. Maeda, and H. Terauchi, J. Phys. Condens. Matter **6**, 9317 (1994).
[36] A. Kodre, I. Arčon, J. Padežnik Gomilšek, and B. Zalar, *X-Ray Absorption Fine Structure-XAFS13*, edited by B. Hedman and P. Pianetta (Springer, Berlin, 2007), p. 120; D. Cabaret, B. Couzinet, A.-M. Flank, J.-P. Itié, P. Lagarde, and A. Polian, *X-Ray Absorption Fine Structure-XAFS13*, edited by B. Hedman and P. Pianetta (Springer, Berlin, 2007), p. 241.
[37] E. Bousquet and P. Ghosez, Phys. Rev. B **74**, 180101(R) (2006).
[38] I. A. Kornev and L. Bellaïche, Phase Transit. **80**, 385 (2007).